



GLOBAL JOURNAL OF RESEARCHES IN ENGINEERING: A
MECHANICAL AND MECHANICS ENGINEERING
Volume 19 Issue 3 Version 1.0 Year 2019
Type: Double Blind Peer Reviewed International Research Journal
Publisher: Global Journals
Online ISSN: 2249-4596 & Print ISSN: 0975-5861

Influence of Temperature with its Geometric and Failure Morphology Defects on the Mechanical Properties of Graphene: Molecular Dynamics Simulation (MDs)

By Muse Degefe Chewaka Liban & Dr. Prabhu Paramasivam

Mettu University

Abstract- This paper addressed that graphene is a regular monolayer of carbon atoms settled in a 2D-hexagonal lattice; which is listed among the strongest material ever measured with strength exceeding more than hundred times of steel. However, the strength of graphene is critically influenced by temperature, geometric & vacancy defects (VD). Defects are at all believed to worsen the mechanical toughness and reduce the strength of graphene sheet. They are revealed that stiffness and strength are the key factors in determining solidity and life span of any technological devices. Molecular dynamics-based atomistic modeling was performed to predict and quantify the effect of non-bonded interactions on the failure morphology of vacancy affected sheets of graphene. The defective sheet of graphene containing vacancy defect was simulated in conjunction with the non-bonded interactions experienced due to the presence of a pristine sheet of graphene.

Keywords: *graphene, vacancy defects, fracture strength, molecular dynamics simulation, failure morphology.*

GJRE-A Classification: FOR Code: 091399



Strictly as per the compliance and regulations of:



RESEARCH | DIVERSITY | ETHICS

© 2019. Muse Degefe Chewaka Liban & Dr. Prabhu Paramasivam. This is a research/review paper, distributed under the terms of the Creative Commons Attribution-Noncommercial 3.0 Unported License <http://creativecommons.org/licenses/by-nc/3.0/>, permitting all non commercial use, distribution, and reproduction in any medium, provided the original work is properly cited.

Influence of Temperature with its Geometric and Failure Morphology Defects on the Mechanical Properties of Graphene: Molecular Dynamics Simulation (MDs)

Muse Degefe Chewaka Liban ^α & Dr. Prabhu Paramasivam ^σ

Abstract- This paper addressed that graphene is a regular monolayer of carbon atoms settled in a 2D- hexagonal lattice; which is listed among the strongest material ever measured with strength exceeding more than hundred times of steel. However, the strength of graphene is critically influenced by temperature, geometric & vacancy defects (VD). Defects are at all believed to worsen the mechanical toughness and reduce the strength of graphene sheet. They are revealed that stiffness and strength are the key factors in determining solidity and life span of any technological devices. Molecular dynamics-based atomistic modeling was performed to predict and quantify the effect of non-bonded interactions on the failure morphology of vacancy affected sheets of graphene. The defective sheet of graphene containing vacancy defect was simulated in conjunction with the non-bonded interactions experienced due to the presence of a pristine sheet of graphene. In this study, the author also revealed that mechanical properties and failure morphology of single and bi-layer graphene sheets under the influence of single, double, and multi-vacancy defects. It was concluded based on atomistic simulations that non-bonded interactions as well as stiffness of a pristine graphene sheet has a significant impact on the failure morphology of the defective graphene sheet. Non-bonded interactions, in conjunction with defects, can be further used for modifying the brittle nature of graphene to ductile.

Keywords: graphene, vacancy defects, fracture strength, molecular dynamics simulation, failure morphology.

1. INTRODUCTION

Graphene is an outstanding material which has a number of multifunctional properties that repeatedly gross it into the title of “wonder material” which is a road map on the way to guide the community toward the development of products [1]. The remarkable mechanical behavior and properties of graphene-based material's has concerned with important study concern in recent years, in line for to their encouraging forecasts, now adaptable divisions for example micromechanics [2], microelectronics [3], and thermal [4] application with desired mechanical

properties, and electrical conductivities [2-4]. The trial and hypothetical revision of graphene, two-dimensional (2D), is a tremendously growing field of today's condensed matter research. The causes for this massive methodical attention were diverse; on the other hand, one might highlight some key inspirations. Keeping given of the science-based interest generated via graphene and its promising upcoming contribution toward electronic engineering and sensing applications, so a group of research effort is steadfastly hooked on considering the configuration and properties of graphene in this paper. Outstanding toward its excellent mechanical behavior, thermal and electrical conductivities of graphene could also use for more conventional purposes as compared with carbon nanotubes, which was quit restricted to aerospace industries and graphene is also known to have very-high stiffness in addition strength until now an extensive scatter have been witnessed in the mechanical properties [1-4]. In this effort, we present molecular dynamics model simulation for the initiation of defects and the influence of different defects (vacancy defects) and pristine one on mechanical strength of graphene sheets were observed and, the fracture strength was predicted from the numerical simulation and the properties of graphene in table 1 and investigated young's modulus displayed in table 2 below.

Table 1: Properties for a Single Sheet of Graphene [1].

Property	Value
Young's modulus [1]	1.0TPa
Rupture strength [1]	130GPa
Tensile strength [2]	100GPa
Thermal conductivity [3-4]	5000w/mK
Shear modulus [5-6]	280GPa
Longitudinal sound velocity [5,7-9]	20km/s
Melting temperature [5,10]	4900K
Specific surface area [11]	2630m ² /g
Optical transmittance [12]	97.70%
High electron mobility [13]	250,000cm ² /Vs

Author ^α ^σ: Department of Mechanical Engineering, Faculty of Engineering and Technology, Mettu university, Ethiopia (East Africa), po Box 318. e-mails: musemtiitr194@gmail.com, lptprabhu@gmail.com

Table 2: Young's modulus of pristine and defective graphene found by different research

Studied by	Conditions/ Types of Defects	Methods Adopted	Young's Modulus (TPa)	Poisson's Ratio
Jiang et al. ¹⁴	T = 100-500 K	Molecular Dynamics	0.95 - 1.1	0.17
Shen et al. ¹⁵	T = 300-700 K	Molecular Dynamics	0.905	
Lee et al. ¹⁶	Pristine graphene	Experiment	1 ± 0.1	
Tsai et al. ¹⁷	NPT ensemble	Molecular Dynamics	0.912	0.261
Sakhaee-Pour ¹⁸	Pristine graphene	Finite Element Method	1.025	
Georgantzinos et al. ¹⁹	Pristine graphene	Finite Element Method	1.367	
Kvashnin et al. ²⁰	Vacancy defects	Molecular Mechanics	1.08	
Neek-Amal et al. ²¹	randomly distributed vacancy defects	STW defects	0.501 ± 0.032	
Shokrieh et al. ²²	Pristine graphene	Continuum Mechanics	1.04	
R.Ansary et al. ²³	STW defects	Molecular Dynamics	60% reduction	
Muse Degefe & Avinash Parashar et al. ²⁴	Vacancy bi-layer graphene T=300K	Molecular Dynamics	0.91	

II. MODELING AND METHODOLOGY

a) Molecular Dynamics based Simulation

Molecular dynamics-based simulations were performed to study the effect of non-bonded interactions on the mechanical behavior and failure morphology of defective graphene sheet. The success of any molecular dynamics-based simulations entirely depends on the interatomic potentials chosen for simulating the atomic interactions. A Significant amount of advancement in conjunction with computational techniques has already been made by the researchers

$$E^{AIREBO} = \frac{1}{2} \sum_i \sum_{j \neq i} \left[E_{ij}^{REBO} + E_{ij}^{LJ} + \sum_{k \neq i, j} \sum_{l \neq i, j, k} E_{kij}^{ltors} \right] \quad (1)$$

Here, i, j, k, and l refers to individual atoms, E is the total potential energy of the system estimated with the help of AIBO potential. To perform this study, a graphene sheet consisting of 800 atoms was generated in the simulation box. The dimensions of a single sheet of graphene was kept fixed at A=46.599Å and B=49.19Å (as shown in Fig.1) along the zig-zag and arm chair direction respectively. In-plane periodic boundary conditions were imposed on the simulation performed at such a low temperature of 1K. Stress-strain response was estimated in this study with the help of the virial stress component [26, 27], which can be

$$\sigma_{ij}^{\alpha} = \frac{1}{V} \left(\frac{1}{2} m^{\alpha} v_i^{\alpha} v_j^{\alpha} + \sum_{\beta=1, n} r_{\alpha\beta}^j f_{\alpha\beta}^i \right); \quad (2)$$

Here, i and j denote indices in Cartesian coordinates system; α and β are the atomic indices; m^{α} and v^{α} are mass and velocity of atom α ; $r_{\alpha\beta}$ is the

in developing potentials for capturing the realistic properties for the range of materials. In this study, AIBO (adaptive intermolecular reactive bond order) potential was used to compute the interatomic forces between carbon atoms in graphene. Simulations were performed with a single cutoff distance of 1.95Å as proposed in the work of [25]. AIREBO potential consists of a summation of pair potential REBO (E_{ij}^{REBO}), non-bonded Lennard Jones potential (E_{ij}^{LJ}) and torsional component between carbon atoms (E_{ijk}^{tors}), also described with the help of mathematical expressions in equation (1).

box. The interlayer spacing between the sheets of graphene in bilayer graphene was kept constant at 3.45Å. During the simulations, the NPT (isothermal-isobaric) ensemble in conjunction with an integration time step of 1fs was enforced. After achieving a minimum energy configuration of graphene, atoms at a temperature of 1K, tensile loading was applied at a strain rate of 0.005ps⁻¹. To avoid thermal effects on the failure mechanism of graphene, simulations were calculated with the help of mathematical expression given in equation (2).

distance between α and β atoms and V is the surrounding volume of atom α .

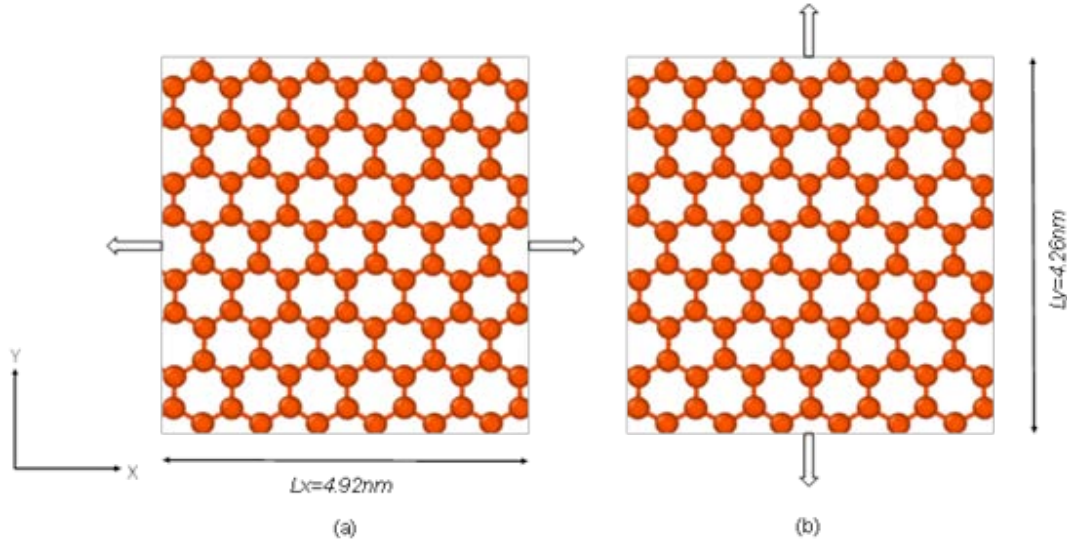


Figure 1: Single graphene sheet: same tension alongside; (a) Zigzag direction and, (b) armchair direction; Simulation models of single graphene sheet where the dimension is given by L_x and L_y : uniaxial tension along.

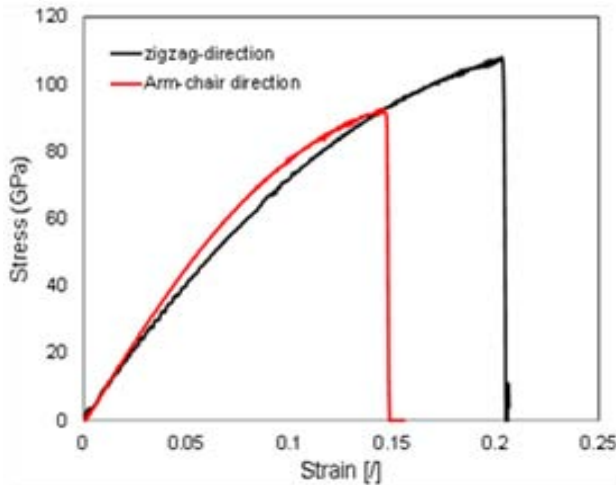


Figure 2: Snapshots on the way to confirm the mathematical method, the fracture strength of a pristine graphene sheet was initially calculated. Stress-strain bends of pristine graphene sheet under same tension along the zigzag way (black color) and armchair way (red color) at 300K.

Now the direction of validating the mathematical method, the rupture stress of pure graphene sheet was initially designed. The Consequence of minimal stress-strain bend next to the temperature of 300 K, subjected to tension load alongside both armchair and zigzag directions shown above Fig.1, was revealed, that fracture stress beside the armchair and the zigzag way are calculated as 91 and 106 GPa, separately. In Cauchy stress; the rupture stiffness was 100GPa and 126 GPa, and the rupture strain is 0.13 and 0.22 correspondingly. These results were promising new examination, i.e., $\sigma_f \approx 130$ GPa and $\epsilon_f \approx 0.25$ [28] as well as previous numerical simulation [29], verifying

dynamism and exactness of our mathematical approach.

Also, graphene can be subjected to a higher temperature at the production stage as well as when graphene-based devices operate at the higher temperature. As we discussed above Chemical vapor deposition (CVD) is one of the most commonly used methods of graphene manufacture; that products graphene at a temperature of around 800 K. Therefore, understanding the temperature behavior of graphene helps to fabricate best excellence graphene founded devices. Studying the effect of high temperature on mechanical properties of a substantial armchair and zigzag is presented. In the temperature range of 200K, 300K, and 450K, the breakage stress with a vacancy was evaluated subjected to load; along with armchair and zigzag way. Modeling was held at a temperature of 200K, 300K, and 450K as shown in Fig.3. (a), and (b) Shows the fracture strength σ_f for the graphene sheets without defect at temperatures of 200 K, 300 K, and 450 K.

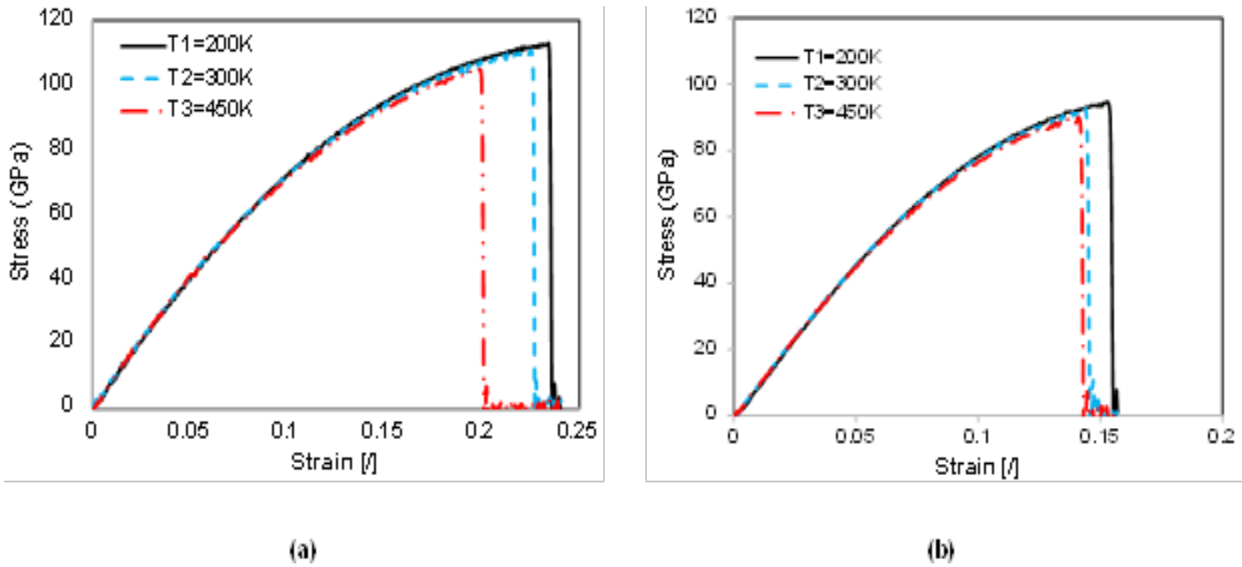


Figure 3: Stress versus strain curves; (a) Zigzag direction graphene sheets at different temperatures, (b) Armchair direction graphene sheets at different temperatures.

III. RESULTS AND DISCUSSION

Molecular dynamics-based simulations were performed to capture the failure morphology of pristine graphene either as a single or in bi-layer sheet configuration. These simulations were performed with the help of three models to study the effects of non-bonded interactions on the mechanical behavior of pristine graphene. Stress and strain response estimated along the zig-zag and arm chair directions of pristine

single sheet graphene were plotted in Fig.4. It can be observed from Fig.4 that the mechanical properties of pristine graphene along with the zig-zag and arm chair directions are quite different because of edge defects. In direction to get a better insight on the failure mechanism of the pristine form of graphene under the influence of tensile loading, snapshots of the simulation box were taken at the time of initiation of the failure as provided in Fig.4.

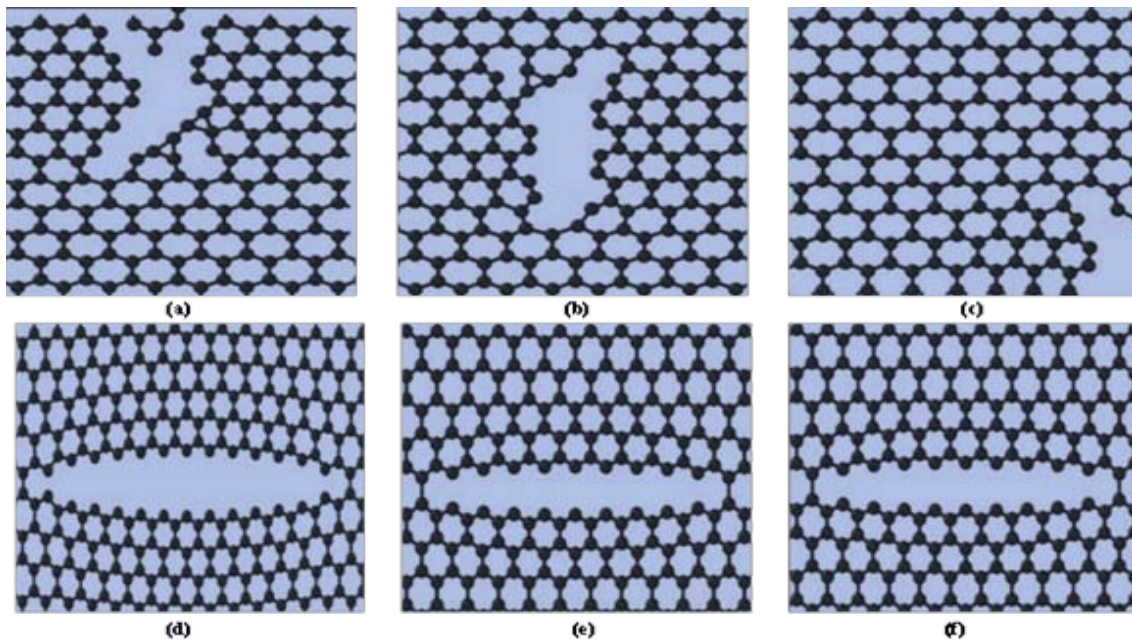


Figure 4: Failure morphology of pristine single and bilayer sheets (a & d) along zig-zag and arm chair directions respectively (b & e) along zig-zag and arm chair directions with non-bonded interactions between bi-layer configuration of graphene containing one defective and another pristine sheet (c & f) along zig-zag and arm chair directions with (bi-layer configuration of graphene containing one defective and another pristine that without non-bonded interactions) [24].

It is observed that the failure morphology of graphene sheet inferred from the snapshots provided in Fig.4 is almost independent of the non-bonded interactions. A brittle nature of failure can be observed in zig-zag as well as arm chair directions of graphene sheets under the influence of tensile loading.

Stress and strain response estimated along with the zig-zag and arm chair directions of pristine single sheet graphene & bi-layer with (LJ-On) & (LJ-Off) were plotted in Fig.5 below. It can be observed from Fig.5 that the mechanical properties of pristine graphene single & bi-layer along the zig zag and arm chair direction.

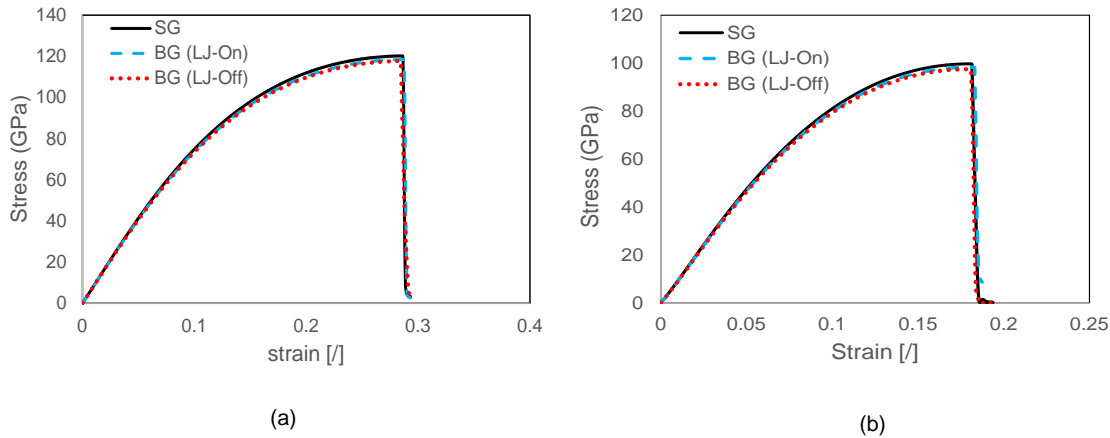
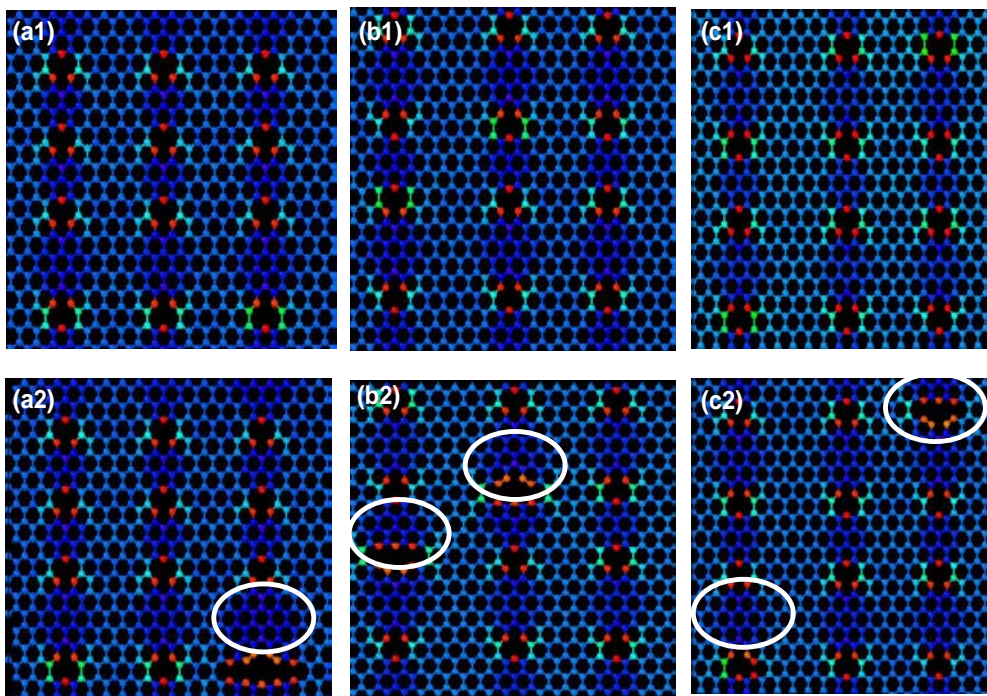


Figure 5: Stress-strain curves of pristine graphene under (a) zigzag and (b) armchair direction; where SG (single graphene sheet), BG (LJ-On) (bilayer graphene sheet with non-bonded interactions) and BG (LJ-Off) (bilayer graphene without non-bonded interactions) [24].

It can be inferred from Fig.6 that non-bonded interactions as well as stiffness of pristine graphene have an impact on the failure morphology of defective graphene sheet containing single vacancy defects. Snapshots of the simulation box provided in Fig.6 (c3) for defective graphene sheet accompanied by a pristine sheet of graphene connected with non-bonded

interactions show that the failure initiates at two different regions subsequently and helps in achieving higher failure strength. This initiation of failure at two different defects helps in distributing the energy among these points, which can be attributed to the higher failure strength for defective graphene sheets in bilayer configuration connected with non-bonded interactions.



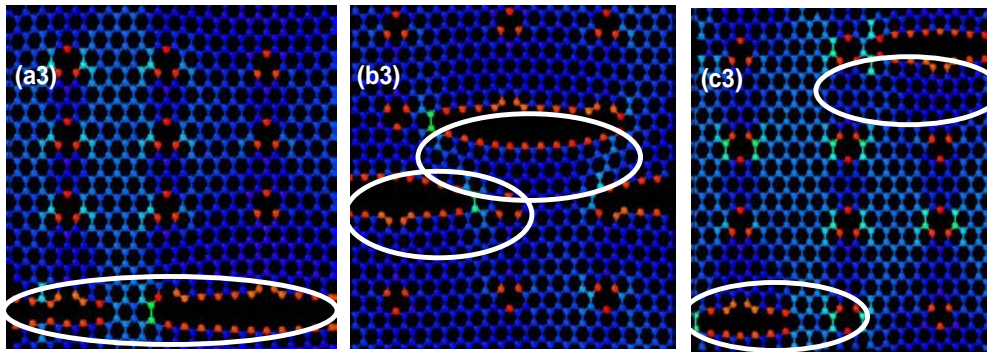


Figure 6: Failure morphology of defective graphene with varying concentration of single vacancy defects in arm-chair direction (a1) initiation of failure in isolated single defective sheet of graphene at 0.5% single vacancy defects (a2) initiation of failure in isolated single defective sheet of graphene at 1.0% single vacancy defects (a3) initiation of failure in isolated single defective sheet of graphene at 1.5% single vacancy defects (b1) initiation of failure in defective sheet of graphene in bilayer sheets connected with non-bonded interactions at 0.5% single vacancy defects (b2) initiation of failure in defective sheet of graphene in bilayer sheets connected with non-bonded interactions at 1.0% single vacancy defects (b3) initiation of failure in defective sheet of graphene in bilayer sheets connected with non-bonded interactions at 1.5% single vacancy defects (c1) initiation of failure in defective sheet of graphene in bilayer sheets without non-bonded interactions at 0.5% single vacancy defects (c2) initiation of failure in defective sheet of graphene in bilayer sheets without non-bonded interactions at 1.0% single vacancy defects (c3) initiation of failure in defective sheet of graphene in bilayer sheets without non-bonded interactions at 1.5% single vacancy defects.

In the way to investigate the reasons behind the improvement in the fracture strength and strain of defective graphene in bilayer configuration of graphene, snapshots at the time of initiation of failure are provided in Fig.7. It can be observed in Fig.6 (b3 and c3) that at the higher concentration of single vacancy defects failure triggers from the vacancies at two separate locations. Distribution of loading with the help of non-bonded interactions as well as pristine graphene sheet accompanied the defective graphene can be attributed to the higher strength of defective graphene in bi-layer sheets of graphene. This subsection of the molecular dynamics based simulation helps in concluding that at higher percentage of single vacancy defects, bilayer sheets of graphene shows higher strength and strain values for the failure of defective graphene sheet. Improvement in the strength of defective sheet was observed in the presence of another pristine graphene connected with non-bonded interactions, but no transition from brittle behavior was observed in any of the failure morphology.

a) Result of single, double and multiple vacancy defects

Failure morphology of the single graphene with uniformly distributed vacancies during strain failure vs vacancy defect ratio was displayed in Fig.7. A very instance concentrated stress occurred near unperfected; at that moment breakages happen to open from were vacancy defect started then growth in the direction of nearby defects where fracture starts

randomly from the defect of vacancies exist. We now turn to analyze the mechanical properties at the failure point for defective graphene. It should be noted that the ultimate strength is the maximum stress in the stress-strain curves, while the fracture strain is determined from the spontaneous large drop of the total energy increment curves. Without defect, the ultimate tensile strength is 91GPa and 106 GPa intended for armchair and zigzag graphene separately.

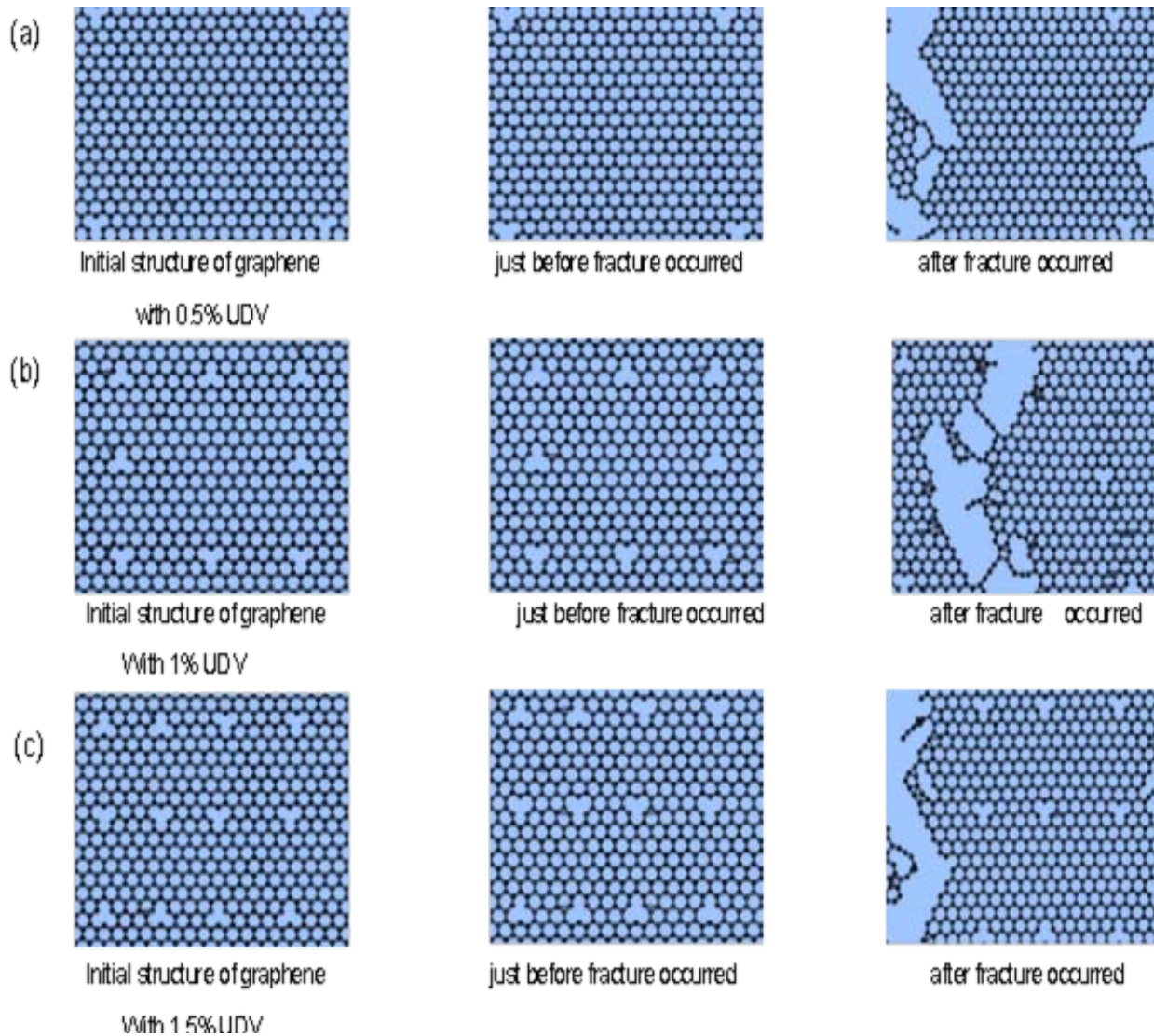


Figure 7: Steps of breakage development in graphene having evenly concentrated vacancies; the vacancy defect ratio was (a) 0.5%, (b) 1%, (c) 1.5%, where, UDV refers to uniformly distributed vacancy defect ratios.

On behalf of through evenly concentrated defects, the correlation among stress, strains besides defects are revealed below Fig.8. (a) & (b). Obviously, the stress decreases with the increase in vacancy defect, and the strain failure decreases with increase vacancy defect. On or after this we decided that in contrast, stiffness to some extent drops by the rising in vacancy Fig. 8 (b) defect; because lack of an atom implies vacancy defect that graphene is more sensitive to vacancy where carbon bond breakage is happens at the time.

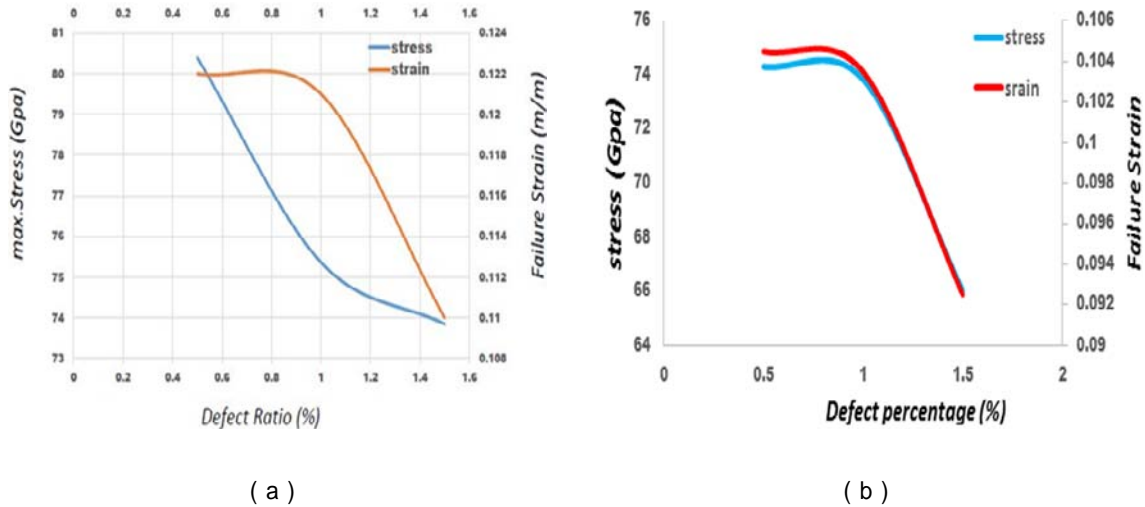


Figure 8: (a) Breakage strong point of unperfected graphene sheet on stress and strain against the number of vacancy defect ratio in Zigzag direction where both lines remain the outcomes of quantized fracture mechanics (QFM). (b) Breakage strong point of an unperfected graphene sheet on stress and strain against the number of vacancy defect ratio in Armchair direction where both lines remain the outcomes of quantized fracture mechanics (QFM).

This study revealed that fracture stress in zig zag direction with different single, double, and multiple vacancy defects are much better in Pristine single graphene than bilayer di-vacancy, single bilayer vacancy

(dangling bond because of odd vacancy defect) and multi-vacancy defect in bilayer single graphene defects are also shown in this bar graph below Fig.9.

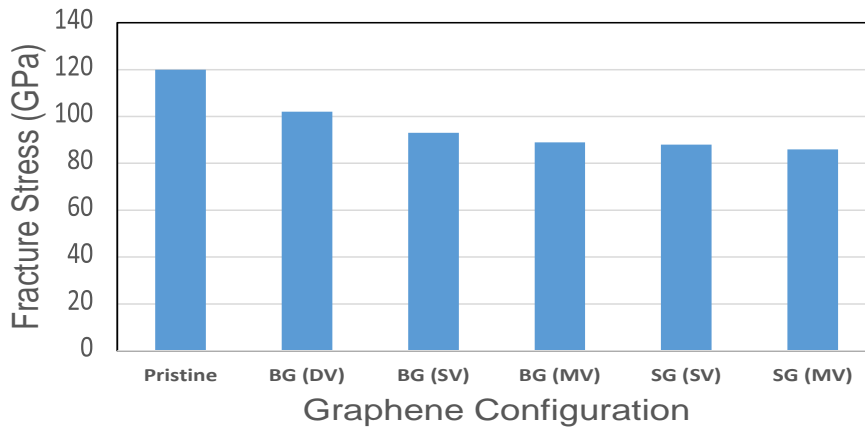


Figure 9: Fracture stress in zig zag direction with different single, double and multiple vacancy defects. Here, the pristine, BG, SG, refers to pristine single graphene sheet, bilayer graphene, and single graphene respectively; Whereas, SV, DV and MV refer to single, di- and multi-vacancy defects.

IV. CONCLUSIONS

Molecular dynamics-based simulations were performed to predict the effect of non-bonded interactions on the mechanical behavior and failure morphology of defective graphene sheet. Simulations were performed with an isolated defective sheet of graphene or defective sheet of graphene accompanied by a pristine sheet of graphene. Atomistic modeling with single as well as bilayer configuration of graphene was performed with different defect concentrations as well as geometries of vacancy defects such as single, double, and multiple vacancy defects. Di-vacancy defects have

predicted higher strength in zig-zag configuration, whereas lower strength in arm chair configuration while compared with the single vacancy defects. A Shift in the failure morphology of graphene along the arm chair direction was observed in bi-layer configuration of defective graphene containing di-vacancy defects. It can be concluded that non-bonded interaction helps in achieving a uniform distribution of load around the defects which triggers the failure simultaneously from different regions & initiating of failure simultaneously from two different points help in achieving a higher strength.

REFERENCES RÉFÉRENCES REFERENCIAS

1. Rajasekeran, G., Prarthana Narayanan, and Avinash Parashar. "Effect of Point and Line Defects on Mechanical and Thermal Properties of Graphene: A Review." *Critical Reviews in Solid State and Materials Sciences* (2015): 1-25.
2. Fennimore, A. M., T. D. Yuzvinsky, Wei-Qiang Han, M. S. Fuhrer, J. Cumings, and A. Zettl. "Rotational actuators based on carbon nanotubes." *Nature* 424, no. 6947 (2003): 408-410.
3. Liu, Bo, C. D. Reddy, Jinwu Jiang, Julia A. Baimova, Sergey V. Dmitriev, Ayrat A. Nazarov, and Kun Zhou. "Morphology and in-plane thermal conductivity of hybrid graphene sheets." *Applied Physics Letters* 101, no. 21 (2012): 211909.
4. Gillen, Roland, Marcel Mohr, Christian Thomsen, and Janina Maultzsch. "Vibrational properties of graphene nanoribbons by first-principles calculations." *Physical Review B* 80, no. 15 (2009): 155418.
5. Mohr, M., J. Maultzsch, E. Dobardž, S. Reich, I. Milošević, M. Damnjanović, A. Bosak, M. Krisch, and C. Thomsen. "Phonon dispersion of graphite by inelastic x-ray scattering." *Physical Review B* 76, no. 3 (2007): 035439.
6. S. V. Dmitriev, J. A. Baimoya, A. V. Savin, Y. S. Kivshar. *Comput. Mater. Sci.* 53 (2012) 194- 203.
7. Los, J. H., Mikhail I. Katsnelson, O. V. Yazyev, K. V. Zakharchenko, and Annalisa Fasolino. "Scaling properties of flexible membranes from atomistic simulations: application to graphene." *Physical Review B* 80, no. 12 (2009): 121405.
8. Novoselov, K. S., D. Jiang, F. Schedin, T. J. Booth, V. V. Khotkevich, S. V. Morozov, and A. K. Geim. "Two-dimensional atomic crystals." *Proceedings of the National Academy of Sciences of the United States of America* 102, no. 30 (2005): 10451-10453.
9. Parashar, Avinash, and Pierre Mertiny. "Multiscale model to investigate the effect of graphene on the fracture characteristics of graphene/polymer nanocomposites." *Nanoscale research letters* 7, no. 1 (2012): 1-8.
10. H. M. Tu, S. H. Huh, S. H. Choi, and H. L. Lee structures of thermally and chemically reduced graphenes, *Mater-lett*, 64 (2010).
11. Lv, Wei, Min Guo, Ming-Hui Liang, Feng-Min Jin, Lan Cui, Linjie Zhi, and Quan-Hong Yang. "Graphene-DNA hybrids: self-assembly and electrochemical detection performance." *J. Mater. Chem.* 20, no. 32 (2010): 6668-6673.
12. A. W. Cummings, D. L. Duong, V. L. Nguyen, D. V. Tuan, J. Kotakoski, J. E. B. Varga, Charge Transport in Polycrystalline Graphene: Challenges and Opportunities, *Adv. Mater.*, 26, 5079-5094.
13. J. L. Tsai, J. F. Tu, Characterizing mechanical properties of graphite using molecular dynamics simulation, *Mater. Des*, 31, 194-199 (2010).
14. Z. Ni, H. Bu, M. Zou, H. Yi, K. Bi, Y. Chen, Anisotropic mechanical properties of graphene sheets from molecular dynamics, *Physica B*, 405, 1301-1306 (2010).
15. Parashar, P. Mertiny, Representative volume element to estimate buckling behavior of graphene/polymer nanocomposites, *Nanoscale Res. Lett.*, 7, 515 (2012).
16. Novoselov, K. S., D. Jiang, F. Schedin, T. J. Booth, V. V. Khotkevich, S. V. Morozov, and A. K. Geim. "Two-dimensional atomic crystals." *Proceedings of the National Academy of Sciences of the United States of America* 102, no. 30 (2005): 10451-10453.
17. Parashar, Avinash, and Pierre Mertiny. "Multiscale model to investigate the effect of graphene on the fracture characteristics of graphene/polymer nanocomposites." *Nanoscale research letters* 7, no. 1 (2012): 1-8.
18. H. M. Tu, S. H. Huh, S. H. Choi, and H. L. Lee structures of thermally and chemically reduced graphenes, *Mater-lett*, 64 (2010).
19. An, F. P., J. Z. Bai, A. B. Balantekin, H. R. Band, D. Beavis, W. Beriguete, M. Bishai et al. "Observation of electron-antineutrino disappearance at Daya Bay." *Physical Review Letters* 108, no. 17 (2012): 171803.
20. C. Lee, X. Wei, J. W. Kysar, and J. Hone, Measurement of the elastic properties and intrinsic strength of monolayer graphene, *Science* 321, 38–388 (2008).
21. W. Frank, D. M. Tanenbaum, A. M. van der Zande, and P. L. Mc Euen, Mechanical properties of suspended graphene sheets, *J. Vac. Sci. Technol. B* 25, 2558–2561 (2007).
22. W. Jiang, J. S. Wang, and B. Li, Young's modulus of Graphene: a molecular dynamics study, *Phys. Rev. B Condens. Matter* 80, 1660 113405 (2009).
23. L. Shen, H. S. Shen, and C. L. Zhang, Temperature-dependent elastic properties of single layer graphene sheets, *Mater. Des.* 31, 4445–4449 (2010).
24. Degefe, M., & Parashar, A. (2016). Effect of non-bonded interactions on failure morphology of a defective graphene sheet. *Materials Research Express*, 3(4), 045009.
25. C. Lee, X. Wei, J. W. Kysar, and J. Hone, Measurement of the elastic properties and intrinsic strength of monolayer graphene, *Science* 321, 38–388 (2008).
26. Sakhaee-Pour, Elastic properties of single-layered graphene sheet, *Solid State Commun.* 149, 91–95 (2009).
27. M. Neek-Amal and F. M. Peters, Linear reduction of stiff-ness and vibration frequencies in defected



circular monolayer graphene, Phys. Rev. B Condens. Matter 81, 235437 (2010).

28. M. Shokrieh and R. Rafiee, Prediction of Young's modulus of graphene sheets and carbon nanotubes using nanoscale continuum mechanics approach, Mater. Des. 31, 790–795 (2010).
29. R. Ansari, S. Ajori, and B. Motevalli, Mechanical properties of defective single-layered graphene sheets via molecular dynamics simulation, Super lattices Microstructure. 51, 274–289 (2012).